

Composite Ni-TiO₂ nanotube arrays electrode for photo-assisted electrolysis

Alfonso Pozio^{*1}, Amedeo Masci¹ and Mauro Pasquali²

¹ENEA, C.R. Casaccia, Via Anguillarese 301, 00123 - S. Maria di Galeria, Rome, Italy

²University of Rome "La Sapienza" - Via del Castro Laurenziano 7, 00161 Rome, Italy

(Received August 6, 2014, Revised February 27, 2015, Accepted April 29, 2015)

Abstract. This article is addressed to define a new composite electrode constituted by porous nickel and an array of highly ordered TiO₂ nanotubes obtained by a previous galvanostatic anodization treatment in an ethylene glycol solution. The electrochemical performances of the composite anode were evaluated in a photo-electrolyser, which showed good solar conversion efficiency with respect to the UV irradiance together with a reduction of energy consumption. Such a combination of materials makes our system simple and able to work both in dark and under solar light exposure, thus opening new perspectives for industrial-scale applications.

Keywords: nanotube; TiO₂; water photoelectrolysis; photoelectrode; OER

1. Introduction

The photo-generation of hydrogen from the splitting of water using sun energy has been an objective of scientists since the early 1970s when Fujishima and Honda (1972) reported the generation of hydrogen and oxygen in a photo electrochemical cell (PEC) using a TiO₂ electrode irradiated with near UV light.

The publication of the fundamental work of Gong *et al.* (2001), in which the authors created the basis for the development of a new synthesis model for the titania nanotubes based on the anodic oxidation of a titanium foil in fluoride based solutions, opened the way to a new methodology able to combine a simplicity of preparation of the material with a complete control of physical characteristics of the nano-system (Mor *et al.* 2003, Cai *et al.* 2005, Kontos *et al.* 2009, Mor *et al.* 2005a). Besides, being its particular geometric shape particularly appropriate for an application as photo-anode in water-photoelectrolysis (Grimes *et al.* 2008), many studies have been directed towards this field, which have arrived to report elevated values of UV photoconversion efficiency for these nanosystems (Shankar *et al.* 2007, Mura *et al.* 2010). In the meanwhile, a large range of different applications for this material has been discovered. In fact, for example, it is reported that the electrical resistance of the titania nanotubes was highly sensitive to the chemisorbed hydrogen molecules hydrogen sensing (Varghese *et al.* 2003a, Varghese *et al.* 2003b), creating a new route in the hydrogen sensing research field (Chen *et al.* 2008, Sennik *et al.* 2010). But, many other

*Corresponding author, Ph.D., E-mail: alfonso.pozio@enea.it

similar examples of the wide versatility of the TiO₂ nanotube arrays are available in literature, as the dye-sensitized solar cells (Mor *et al.* 2007, Mor *et al.* 2010, Wang *et al.* 2010, Alivov and Fan 2010, Liu and Misra 2010), lithium batteries (Fang *et al.* 2008) and also in different biological and medical researches, like the osteoblast growth (Oh *et al.* 2005, Oh and Jin 2006, Oh *et al.* 2008, Das *et al.* 2008) or drug elution (Popat *et al.* 2007a, b, Peng *et al.* 2009). As regards the application of the TiO₂ nanotube arrays as photo-electrodes for water photoelectrolysis, it is important to emphasize that although many important results have been reached in this field, the commercialization of such nano-system is still far because of the high band gap of titania, which limits the light adsorption only to limited UV region (Grimes *et al.* 2008). In addition, also the titania electro-catalytic activity for the oxygen evolution reaction (*OER*) is very low if compared with that obtained on conventional metallic electrodes (Pt, Ni etc). These problems limit the use of this material due to the low current density produced both in conventional mode or photo-assisted. For this reason, it can be useful a different strategy based on the use of a composite electrode able to guarantee a high electrocatalytic activity for the O₂ evolution but exploiting the photo-activity in order to decrease the power consumption. This type of electrode could be used in a photo assisted electrolyser in a presence of a UV solar light source. In the past, most researchers focused their attention on the doping of TiO₂ nanostructures mainly in order to shift the light adsorption to lower energy region (Wang *et al.* 2006, Ghicov *et al.* 2006a, b, Shankar *et al.* 2006, Li and Shang 2009, Dong *et al.* 2009, Xu *et al.* 2010, Park *et al.* 2006, Raja *et al.* 2006, Wu *et al.* 2007, Mohapatra *et al.* 2007, Hahn *et al.* 2007, Lu *et al.* 2008, Su *et al.* 2008). As alternative, the use of co-catalyst to enhance reactivity was first observed for the photo-conversion of H₂O to H₂ and O₂ using the Pt-TiO₂ system. (Linsebigler *et al.* 1995). The addition of metals to a semiconductor can change the photocatalytic process by changing the semiconductor surface properties. The metal can enhance the yield of a particular product or the rate of the photocatalytic reaction. On the other side, the metal can be important also because of its own electro-catalytic activity. Representative water oxidation inorganic catalysts include nickel oxide, ruthenium oxide, cobalt oxide and iridium oxide, etc (Yang *et al.* 2013). Deposition of NiO_x, IrO_x, CoO_x and RuO_x co-catalysts on n-semiconductors seem all enhance the activity for O₂ evolution. and Ni and Co oxides were found to be the best catalysts in alkaline environment (Surendranath *et al.* 2010, Dincă *et al.* 2010). As example, Dincă *et al.* (2010) described the self-assembly of a highly active nickel-based oxygen evolving catalyst that forms as a thin film on inert electrodes when aqueous solutions of Ni²⁺ salts are electrolyzed in presence of phosphate or borate. These authors evidenced that this catalyst can be formed in situ under mild conditions on a variety of conductive substrates and it exhibits high activity for *OER* at room temperature. The catalyst exhibits long-term stability in water with no observed corrosion permitting energy storage to be performed with devices that are inexpensive and with a high manufacturability. In the past, Shrestha *et al.* (2010) loaded self-organized TiO₂ nanotubes grown by anodization of Ti-substrate in glycerol-water electrolyte containing fluoride with Ni oxide nanoparticles by a simple chemical bath precipitation technique. The synergy of the metal and semiconductor components is important for improving the performance of nanocomposites in photocatalytic applications (Kamat *et al.* 2002).

In the past, to improve the efficiency and reduce the cost of the solar hydrogen production processes, photovoltaic (PV) and electrolyzer were assembled into one integrated unit in which the light-harvesting solar cell is one of the electrodes. The potential advantages of this kind of PEC over PV-electrolysis units included: reduced cost by manufacturing PEC device panels as one unit without interconnections between PV cells, eliminating the separate electrolyzer unit, increasing efficiency by using a very low current density on the electrodes, and providing a system that is

easily scaled up to larger sizes (Kelly and Gibson 2006). In most articles (Sakthivel and Kisch 2003, Lin and Huang 2006, Kelly and Gibson 2006), these kind of PECs were based on triple-junction amorphous silicon (a-Si) solar cell as anode and Ni or Pt as cathode. The PECs showed high efficiency but also strong corrosion problem (Sakthivel and Kisch 2003, Yamada *et al.* 2003, Kaselev *et al.* 2001).

In this article we investigated a different approach, the mechanically coupling of semiconductor/metal in order to produce a metal-semiconductor anode with large area. We inserted TiO₂ nanotubes grown by anodization of Ti-substrate in ethylene glycol electrolyte containing fluoride, directly into porous nickel sheet using a cold pressing method. The result was a PEC with an innovative design in which the anode is constituted by a composite electrode constituted by an array of TiO₂ nanotubes embedded on porous nickel. Such coupling should allow exploiting the electro-catalytic property of Nickel for O₂ evolution together with the photo-catalytic one of TiO₂. We have found that composite Nickel-TiO₂/Ti could represent a valid alternative able to ensure the functioning of the anode in mode photo-assisted (presence of UV) or conventional (without UV).

2. Experimental

2.1 Materials and photo-electrode preparation

Small disks of commercially pure grade-3 titanium (Titania, Italy) have been used as substrate for the nanotube growth. A single circular sample had a diameter of 15 mm with a thickness of 0.5 mm, and was arranged to show an active circular area of 1 cm². The samples (TiO₂/Ti) were prepared with the methodology previously developed in different articles (Mura *et al.* 2009, 2010). Briefly, after 3 min. pickling in a HF (Carlo Erba)/HNO₃ (Carlo Erba) solution made by a volumetric ratio of 1:3 and diluted in deionised water until to 100 ml, the titanium disks have been set in a three-electrode cell containing a 1 M KOH solution (Carlo Erba) and subjected to a prefixed and optimized density current (1 mA/cm²) generated by a potentiostat/galvanostat (Solartron 1286) for 3 min. The counter-electrode was a platinum sheet, while the reference was a standard calomel electrode (SCE). The anodic growth of the nanotube arrays has been obtained in a two-electrode cell with a platinum counter electrode, using a glycol ethylene (Ashland) solution with 1 %wt. H₂O and 0.2 %wt. NH₄F and applying 60 V for 3 h by means of a potenziostat/galvanostat PS251-2 (Aldrich). The current has been measured with a Keithley 2000 multimeter and been acquired with a Madge-Tech Volt101 digital recorder placed in series with a calibrated resistance (300 Ω) Leeds and Northrup (Fig. 1).

After the anodization, the sample was washed in glycol ethylene and left overnight in a dry room. In order to transform amorphous TiO₂ nanotubes obtained by anodic growth into the anatase phase, which shows a higher photo sensibility, after a pre-heat treatment at 90°C in vacuum for 3 hours, the sample has been placed in a tubular furnace (Lenton) for 1 h at 580°C with a slope of 1°C/min in air. A deep characterization of this kind of photo anode (TiO₂/Ti) was already published in previous articles (Mura *et al.* 2009, 2010, Pozio 2014, 2015). Sixteen TiO₂/Ti samples were embedded in a porous nickel sheet. The titanium disks were placed on a 50 cm² foil of porous, ductile nickel (2 mm thickness) and embedded to cold, by applying a pressure of 50 bars by means of a hydraulic press (ATS Faar). The final result was a 16-TiO₂/Ti disk well framed inside the porous structure as shown in Fig. 2(a).

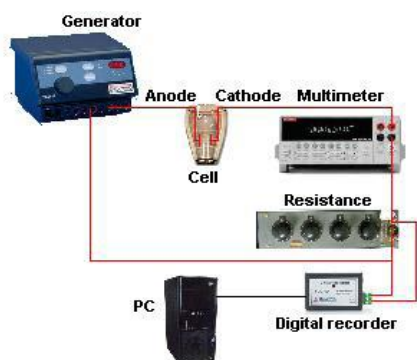


Fig. 1 Scheme of anodization system

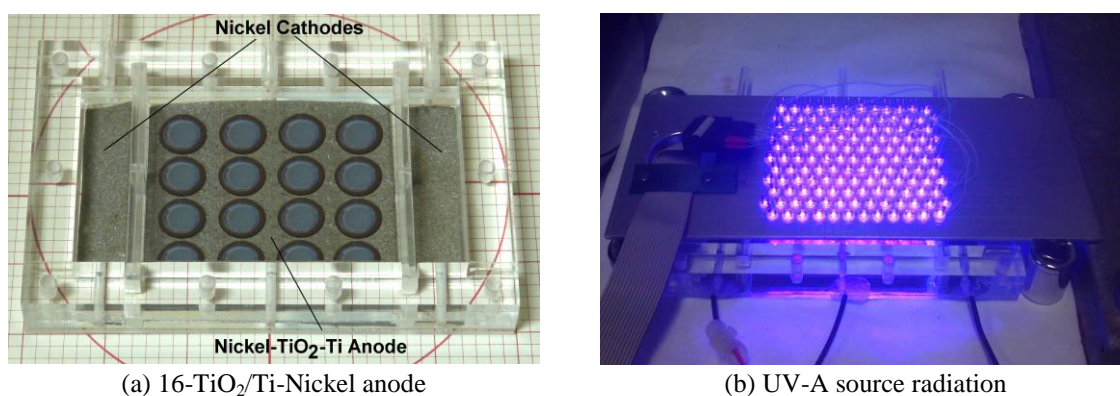


Fig. 2 Photo-electrolysis cell

2.2 Electrochemical measurements

The electrochemical measurements on the composite 16-TiO₂/Ti-Nickel sample were performed using a Plexiglas cell (30 cm³) showed in Fig. 2(a). Measures of photo-electrolysis assisted by UV (Fig. 2B) or without UV (dark) were performed on the cell, between 1.4 to 2.0 V, in a configuration with two electrodes (sample working/Ni counter) in KOH 1 M electrolyte at 25°C.

The anodic and cathodic compartments were separated with a porous gas-proof felt (Testori-Italy). An UV source radiation was provided in an artificial way exposing the cell to a source consisting of an array consisting of 137 LED UV5TZ-390-30 (Bivar) inserted on a card in parallel rows to 6 mm distance between them (Fig. 2(b)). The card was oriented parallel to the surface of the anode and at a distance of 4 cm from the same. The LEDs were powered at a constant current of 10 mA individually emitting a radiation in the UV-A with a relative intensity of 0.5. The overall radiation source was measured by a photo radiometer HD2302 (Delta-Ohm) placing the sensor in the housing of the work cell. The radiation measured in the range 315÷400 nm was equal to 62 W m⁻², this value was independent of the distance card-anode in the range 3÷9 cm and homogeneous on various points of the anode. In addition, the composite electrode was tested during the photo-electrolysis with direct solar light exposition along a whole day. In this case, the photocurrent measurements were carried out by exposing the cell to direct sunlight, measuring the visible

radiation and its UV-A component by means of a photo radiometer HD2302 (Delta-Ohm).

2.3 UV-vis absorption spectra

The diffuse reflectance spectrum of a single TiO₂/Ti sample disk was obtained using a Lambda 9 spectrophotometer equipped with an integrating sphere. The reflectance data was converted to the absorption coefficient $F(R_{\infty})$ values according to the Kubelka-Munk equation (Dupuis and Menu 2006, Simmons 1975)

$$F(R_{\infty}) = \frac{(1 - R_{\infty})^2}{2R_{\infty}} \quad (1)$$

The absorption coefficient $F(R_{\infty})$ and the bandgap E_g are related through the equation (Yoldas and Partlow 1985)

$$[F(R_{\infty}) * h\nu]^s = h\nu - E_g \quad (2)$$

where ν is the frequency, h is the Planck's constant, and $s=0.5$ for indirect bandgap material (Grimes *et al.* 2008). In this way, the plotting of $[F(R_{\infty}) * h\nu]^{0.5}$ vs. $h\nu$, the so-called Tauc plot, gives the possibility to obtain the optical band-gap by dropping a line from the maximum slope of the curve to the x-axis (Mor *et al.* 2005b, Burgeth and Kisch 2002, Yamada *et al.* 2003, Khaselev *et al.* 2001).

3. Results and discussion

3.1 Analysis of the absorbance spectra.

The energy of band gap (E_g) of a single TiO₂/Ti sample disk was calculated using the Tauc plot (Fig. 3), as previously described, obtaining a value of 3.096 eV corresponding to a wave length of 413 nm.

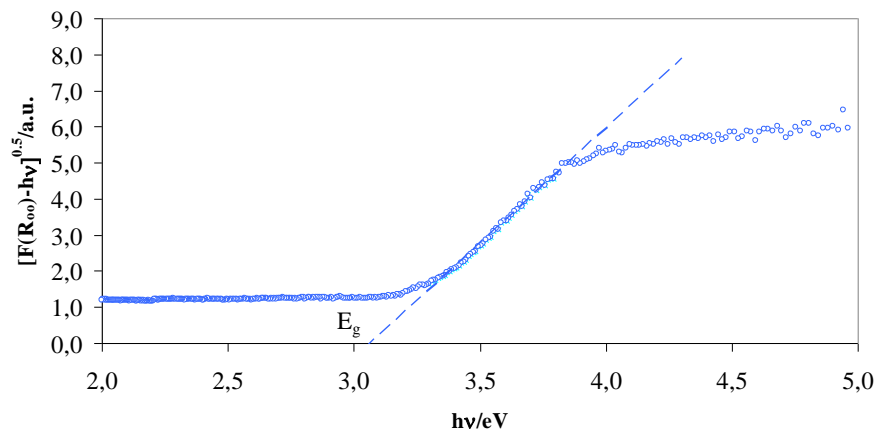


Fig. 3 The transformed Kubelka-Munk function vs. energy of excitation source for TiO₂/Ti (○)

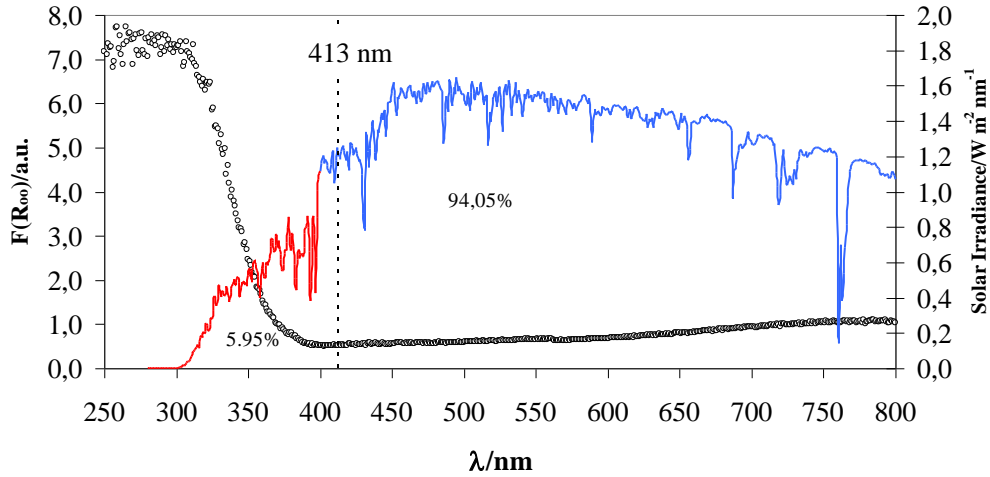


Fig. 4 Absorption coefficient spectra of the TiO_2/Ti (\circ) according to the Kubelka-Munk equation and global solar irradiance in UV (—) or Visible (—) (Grimes *et al.* 2008)

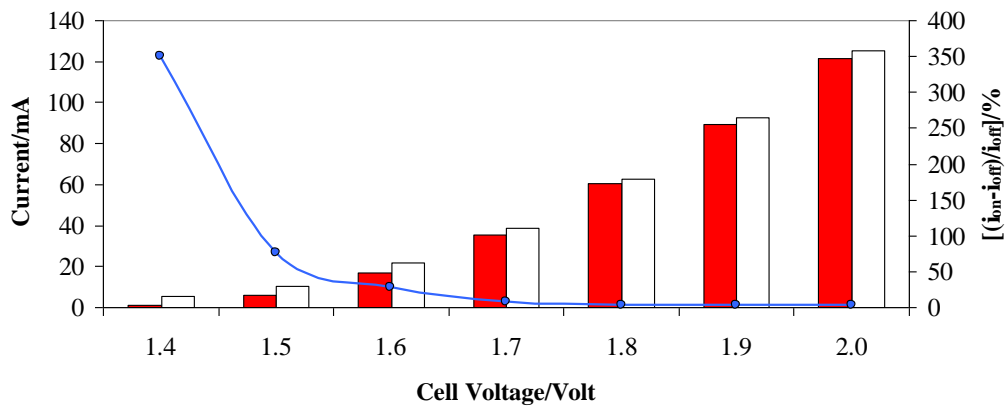


Fig. 5 Current density vs cell voltage with nickel- TiO_2/Ti anode at UV-on (\square) and UV-off (\blacksquare) and relative change of current density (— \bullet —) in KOH 1 M at 25°C, UV intensity 62 W m^{-2}

The diffuse absorbance spectra of a Ti/TiO_2 sample, obtained by the Kubelka-Munk equation, are showed in Fig. 4 together with the global solar irradiance (Grimes *et al.* 2008). The sample can absorb for $\lambda \leq 413 \text{ nm}$ with the main absorbance in the UV range $300 \div 400$ that correspond to about 5.95 % of solar global irradiance (among $300 \div 1050 \text{ nm}$). In the visible range $400 \div 413 \text{ nm}$, only a very small part (1.95 %) of the global solar irradiance (94.05 %) can be absorbed.

3.2 Analysis of the photo-electrolysis cell performance

Fig. 5 shows the electrolysis current obtained at different cell voltages between 1.4-2.0 Volts under conditions of UV on and off and the relative change of current with respect to the value i_{off} .

The measurement shows that using the anode composite Nickel- TiO_2/Ti within an electrolyser, it can generate a photo-additional current so as to produce hydrogen even at very low values of

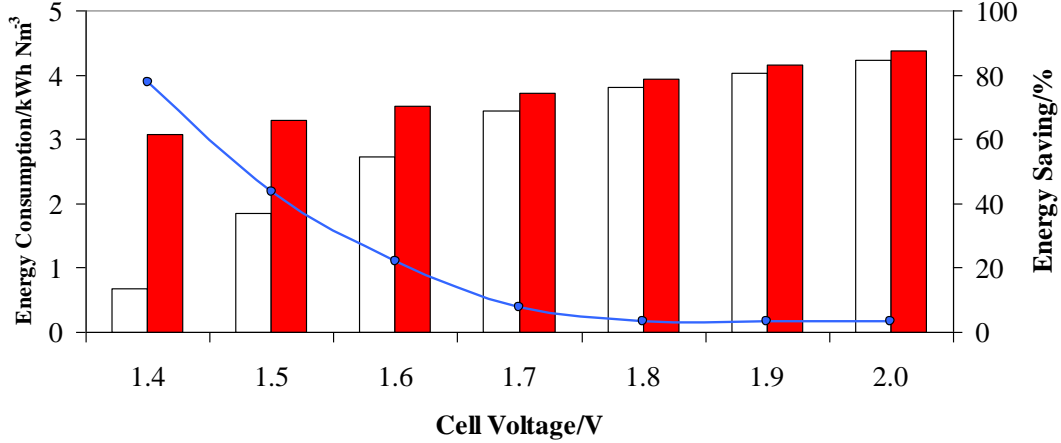


Fig. 6 Energy consumption vs cell voltage with Nickel-TiO₂/Ti anode at UV-on (□) and UV-off (■) and relative energy saving (-●-) in KOH 1 M at 25°C, UV intensity 62 W m⁻²

voltage (i.e., to 1.4 V). Particularly, the onset's voltage of the electrolysis was decreased for about 100 mV, from 1.5 at 1.4 Volt in presence of UV-A light. The efficiency of a hydrogen generator can be evaluated through the amount of energy consumed per cubic meter of hydrogen produced under conditions of standard temperature and pressure. In such conditions, a conventional electrolyser with an efficiency of 100% ($V_{Bias}=1.23$ Volt) has an ideal energy consumption of about 2.7 kWh m⁻³. With increasing applied voltage (V_{Bias}) the power consumption increases proportionately. An electrolyser will have an energy consumption in kWh equal to

$$P = \frac{i_{off} V_{Bias}}{1000} \quad (3)$$

where i_{off} is the electrolysis current. For a photo-electrolyser, the energy consumption is always expressed by Eq. (3), which considers only the current supplied from the external generator (i_{off}), while the volume of hydrogen produced in cubic meters will instead be given by the expression

$$V(H_2) = \frac{i_{on} 3600}{2F} RT \quad (4)$$

where the faradic yield is given by the total current (i_{on}), F is the Faraday's constant and T the temperature (°K). Therefore, the energy consumption of the photo-electrolyser, expressed in kWh m⁻³ will be given by the expression

$$U(H_2) = \frac{P}{V(H_2)} = 2.19 \frac{i_{off} V_{bias}}{i_{on}} \quad (5)$$

where all parameters are measured experimentally. From the Eq. (5) it is observed that in the case in which the electrolyser is not illuminated, the power consumption is simply given by the product of the voltage applied to the constant 2.19. If there is photo-current, consumption will decrease in proportion to the decrease of the ratio i_{off}/i_{on} . The value of the constant, of course, depends inversely on the temperature (2.02 to 50 °C and 2.39 at 0 °C) and directly by the pressure (4.38 to

2 bar abs). The energy consumption of the cell per m^3 of H_2 produced in standard conditions (Eq. (5)) was calculated as a function of the voltage applied to the cell in photo mode assisted and conventional. Fig. 6 shows that the maximum energy saving occurs at low voltage and tends to decrease asymptotically with increasing this up to approx. 3.5% to 2 V. Based on the results obtained we proceeded to perform measurements in conditions of direct exposure to sunlight at two voltages defined, 1.5 and 1.6 V, which are most visible effects photo-electrolytic.

Fig. 7 shows the electrolysis current obtained at a cell voltage of 1.5 V as a function of time under conditions of exposure to direct sunlight, and the same current registered by shielding the cell. The figure also shows the UV-A intensity during the time. The trend evidences a maximum current in the central hours of the morning corresponding to the UV-A maximum. The UV-A radiation intensity, was between $14.0 \div 24.5 \text{ W m}^{-2}$, representing approximately 3% of the incident global radiation.

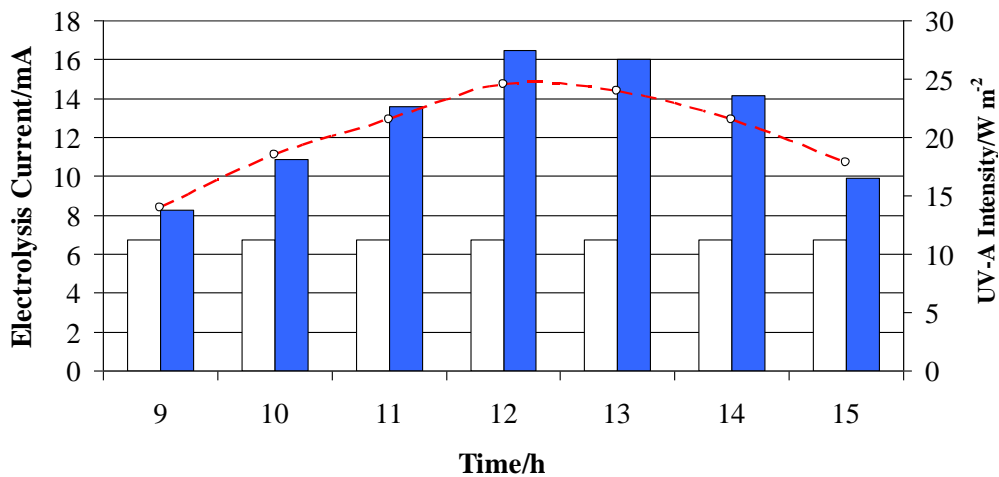


Fig. 7 Electrolysis current vs time with direct solar exposition (■) or dark (□) and UV-A intensity (-○-) in KOH 1 M at 25°C at 1.5 Volt

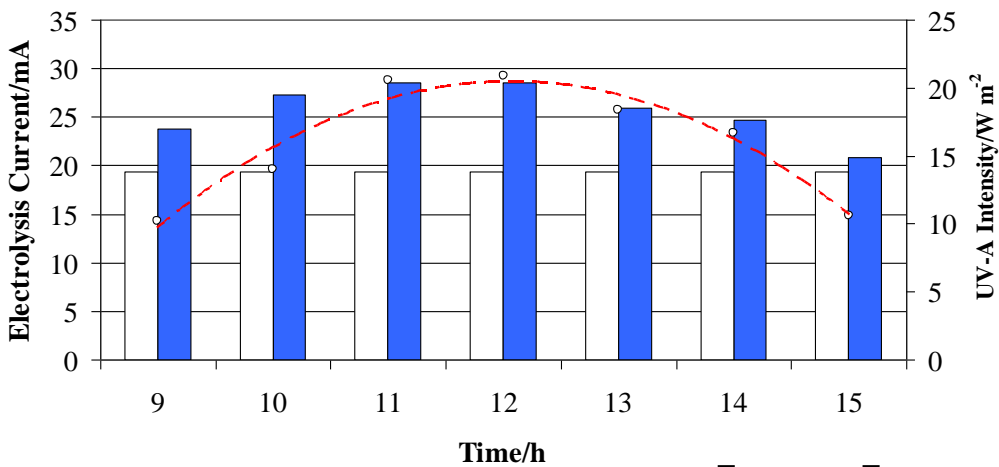


Fig. 8 Electrolysis current vs time with direct solar exposition (■) or dark (□) and UV-A intensity (-○-) in KOH 1 M at 25°C at 1.6 Volt

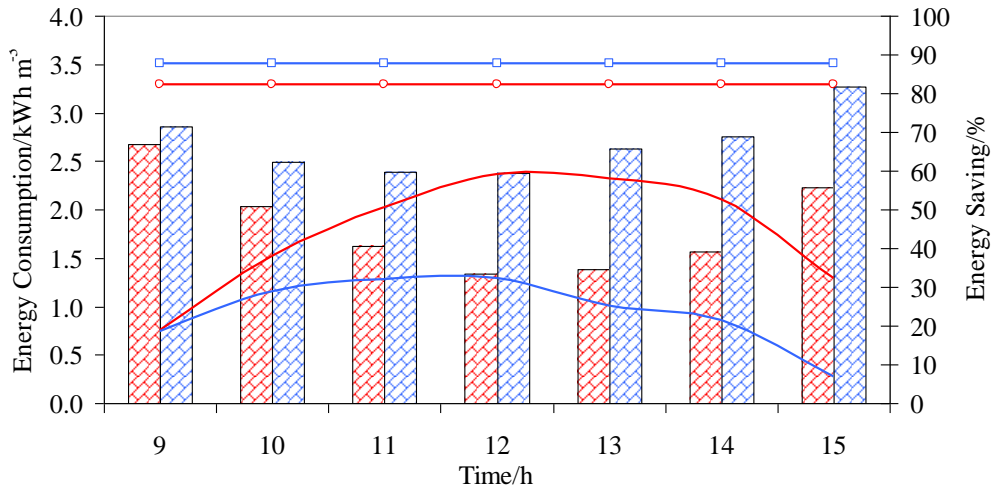


Fig. 9 Photo-electrolyser energy consumption for m³ of H₂ at 1.5 V (▨) or 1.6 V (▩) under direct solar exposition and relative energy saving (— or —). Dashed lines represent the energy consumption in dark at 1.5 V (3.29 kWh m⁻³) (---) and at 1.6 V (3.51 kWh m⁻³) (---)

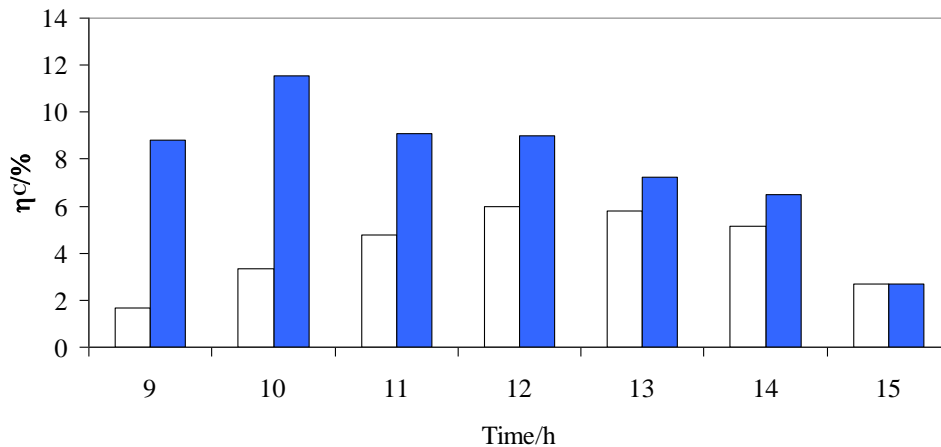


Fig. 10 Solar conversion efficiency vs time with direct solar exposition at 1.5 V (□) and 1.6 V dark (■) in KOH 1 M at 25°C

The same measurements were repeated at a cell voltage of 1.6 V (Fig. 8). The total current in this case was obviously higher in what has increased the potential of electrolysis. Also in this case one observes the maximum of photo-current in the central hours of the morning at the maximum intensity of the UV radiation. The UV-A radiation intensity in this test was lower and between 10.2–20.5 W m⁻², but always represents about 3% of the incident global radiation.

Finally, for both tests was obtained the energy consumption of the system per m³ of H₂ produced in standard conditions (Eq. (5)), as a function of the voltage applied to the cell and in photo mode assisted or conventional (Fig. 9). The graph also shows the reference value of energy consumption always evaluated in standard conditions and in the absence of illumination at 1.5 V and 1.6 V which is equal respectively to 3.29 kWh m⁻³ and 3.51 kWh m⁻³.

It is observed that the increase of light radiation produces an increase in the saving of energy, which is maximum in the central day hours and between 30÷60% depending on the voltage applied to the PEC. In addition, the solar conversion efficiency η_c for the photo-electrolysers was calculated by the following expression (Grimes *et al.* 2008)

$$\eta_c = \frac{i_{ph}(1.23 - V_{bias})}{I_r A} \quad (6)$$

where V_{bias} is the voltage applied to the cell, i_{ph} the photo-current as the difference among i_{on} and i_{off} , A is the irradiated area ($1.8 \times 10^{-3} \text{ m}^2$) and I_r the UV-A irradiance intensity, (W m^{-2}).

The Fig. 10 shows the solar conversion efficiency at V_{bias} of 1.5 and 1.6 volt along the day. In both case, the efficiency show a maximum, respectively 12% at 1.6 V and 6% at 1.5 V. The mean efficiency along the day was 4.2% at 1.5 V and 7.8% at 1.6 V.

4. Conclusions

In this work, we have reported a preliminary study for a new composite electrode constituted by porous nickel and an array of highly ordered TiO_2 nanotubes. The analysis shows that the composite electrode could represent a valid alternative able to ensure the functioning of the anode in either photo-assisted (presence of UV) conventional (without UV). In the case of the composite material, of course, the photo-electrochemical efficiency depends mainly on the component TiO_2/Ti while the support of nickel ensures the catalytic activity in the absence of light.

The measurements carried out show that the cell's design permits a significant step forward in designing a practical photo-electrolysis system for large-scale hydrogen production. The solar conversion efficiency with respect to the UV irradiation was good and the results have evidenced that a photo-electrolyser, operating with a cell voltage of 2 V and with a correct insulation guaranteed by an appropriate design and an optimal management of the gas products could reduce by at least 3.5% its energy consumption. Further analyses are in progress in order to characterize the composite material with respect to its single components.

Acknowledgments

We would thank Dr. Alberto Mittiga of ENEA Utrinn-FVC for the Absorption Spectra measurements.

References

- Alivov, Y. and Fan, Z.Y. (2010), "Dye-sensitized solar cells using TiO_2 nanoparticles transformed from nanotube arrays", *J. Mater. Sci.*, **45**, 2902-2906.
- Burgeth, G. and Kisch, H. (2002), "Photocatalytic and photoelectrochemical properties of titania-chloroplatinate (IV)", *Coord. Chem. Rev.*, **230**, 41-47.
- Cai, Q., Paulose, M., Varghese, O.K. and Grimes, C.A. (2005), "The effect of electrolyte composition on the fabrication of self-organized titanium oxide nanotube arrays by anodic oxidation", *J. Mater. Res.*, **20**(1), 230-236.

- Chen, Q., Xu, D., Wu, Z. and Liu, Z. (2008), "Free-standing TiO₂ nanotube arrays made by anodic oxidation and ultrasonic splitting", *Nanotechnology*, **19**, 365708.
- Das, K., Bandyopadhyay, A. and Bose, S. (2008), "Biocompatibility and in situ growth of TiO₂ nanotubes on Ti using different electrolyte chemistry", *J. Am. Ceram. Soc.*, **91**(9), 2808-2814.
- Dincă, M., Surendranath, Y. and Nocera, D.G. (2010), "Nickel-borate oxygen-evolving catalyst that functions under benign conditions", *PNAS*, **107**(23), 10337-10341.
- Dong, L., Ma, Y., Wang, Y., Tian, Y., Ye, G. and Jia, X. (2009), "Preparation and characterization of nitrogen-doped titania nanotubes", *Mater. Lett.*, **63**(18-19), 1598-1600.
- Dupuis, G. and Menu, M. (2006), "Quantitative characterization of pigment mixtures used in art by fibre-optics diffuse-reflectance spectroscopy", *Appl. Phys. A, Mater. Sci. Proc.*, **83**, 469.
- Fang, D., Liu, S.Q., Chen, R.Y., Huang, K.L., Li, J.S., Yu, C., Qin, D.Y. and Xuebao, W.C. (2008), "Fabrication and characterization of highly ordered porous anodic titania on titanium substrate", *J. Inorg. Mater.*, **23**(4), 647-651.
- Fujishima, A.K. and Honda, K. (1972), "Electrochemical photolysis of water at a semiconductor electrode", *Nature*, **238**, 37-38
- Ghicov, A., Macak, J.M., Tsuchiya, H., Kunze, J., Haeublein, V., Frey, L. and Schmuki, P. (2006a), "Ion implantation and annealing for an efficient N-doping of TiO₂ nanotubes", *Nano Lett.*, **6**(5), 1080-1082.
- Ghicov, A., Macak, J.M., Tsuchiya, H., Kunze, J., Haeublein, V., Kleber, S. and Schmuki, P. (2006b), "TiO₂ nanotube layers: dose effects during nitrogen doping by ion implantation", *Chem. Phys. Lett.*, **419**, 426-429.
- Gong, A., Grimes, C.A., Varghese, O.K., Hu, W., Singh, R.S., Chen, Z. and Dickey, E.C. (2001), "Titanium oxide nanotube arrays prepared by anodic oxidation", *J. Mater. Res.*, **16**, 3331-3334
- Grimes, C.A., Varghese, O.K. and Ranjan, S. (2008), *The Solar Hydrogen Generation by Water Photoelectrolysis*, Springer, New York, NY, USA.
- Hahn, R., Ghicov, A., Salonen, J., Lehto, V.P. and Schmuki, P. (2007), "Carbon doping of self-organized TiO₂ nanotube layers by thermal acetylene treatment", *Nanotechnology*, **18**, 105604.
- Kamat, P., Flumiani, M. and Dawson, A. (2002), "Metal-metal and metal-semiconductor composite nanoclusters", *Coll. Surf. A: Physicochem. Eng. Aspec.*, **202**, 269-279.
- Khaselev, O., Bansal, A. and Turner, J.A. (2001), "High-efficiency integrated multijunction photovoltaic/electrolysis systems for hydrogen production", *Int. J. Hydro. Energy*, **26**, 127-32.
- Kelly, N.A. and Gibson, T.L. (2006), "Design and characterization of a robust photoelectrochemical device to generate hydrogen using solarwater splitting", *Int. J. Hydro. Energy*, **31**, 1658-1673.
- Kontos, A.G., Kontos, A.I., Tsoukleris, D.S., Likodimos, V., Kunze, J., Schmuki, P. and Falaras, P. (2009) "Photo-induced effects on self-organized TiO₂ nanotube arrays: the influence of surface morphology", *Nanotechnology*, **20**(4), 045603.
- Li, Q. and Shang, J.K. (2009), "Self-organized nitrogen and fluorine Co-doped titanium oxide nanotube arrays with enhanced visible light photocatalytic performance", *Environ. Sci. Tech.*, **43**(23), 8923-8929.
- Lin, H., Huang, C.P., Li, W., Ni, C., Ismat, S. and Tseng, Y. (2006), "Size dependency of nanocrystalline TiO₂ on its optical property and photocatalytic reactivity exemplified by 2-chlorophenol", *Appl. Catal. B: Environ.*, **68**, 1-11.
- Linsebigler, A.L., Lu, G. and Yates, J.T. (1995), "Photocatalysis on TiO₂ surfaces: principles, mechanisms, and selected results", *Chem. Rev.*, **95**, 735-758.
- Liu, Z. and Misra, M. (2010), "Bifacial dye-sensitized solar cells based on vertically oriented TiO₂ nanotube arrays", *Nanotechnology*, **21**, 125703(1-4).
- Lu, N., Zhao, H., Li, J., Quan, X. and Chen, S. (2008), "Characterization of boron-doped TiO₂ nanotube arrays prepared by electrochemical method and its visible light activity", *Separat. Purific. Tech.*, **62**, 668-673.
- Mohapatra, S.K., Misra, M., Mahajan, V.K. and Raja, K.S. (2007), "Design of a highly efficient photoelectrolytic cell for hydrogen generation by water splitting: application of TiO_{2-x}C_x nanotubes as a photoanode and Pt/TiO₂ nanotubes as a cathode", *J. Phys. Chem. C*, **111**(24), 8677-8685.
- Mor, G.K., Varghese, O.K., Paulose, M., Mukherjee, N. and Grimes, C.A. (2003), "Fabrication of tapered,

- conical-shaped titania nanotubes”, *J. Mater. Res.*, **18**(11), 2588-2593.
- Mor, G.K., Shankar, K., Paulose, M., Varghese, O.K. and Grimes, C.A. (2005a), “Enhanced photocleavage of water using titania nanotube arrays”, *Nano Lett.*, **5**(1), 191-195.
- Mor, G.K., Varghese, O.K., Paulose, M. and Grimes, C.A. (2005b), “Transparent highly ordered TiO₂ nanotube arrays via anodization of titanium thin films”, *Adv. Funct. Mater.*, **15**, 1291-1296.
- Mor, G.K., Shankar, K., Paulose, M., Varghese, O.K. and Grimes, C.A. (2007), “High efficiency double heterojunction polymer photovoltaic cells using highly ordered TiO₂ nanotube arrays”, *Appl. Phys. Lett.*, **91**, 152111.
- Mor, G.K., Basham, J., Paulose, M., Kim, S., Varghese, O.K., Vaish, A., Yoriya, S. and Grimes, C.A. (2010), “High-efficiency Förster resonance energy transfer in solid-state dye sensitized solar cells”, *Nano Lett.*, **10**(7), 2387-2394.
- Mura, F., Pozio, A., Masci, A. and Pasquali, M. (2009), “Effect of a galvanostatic treatment on the preparation of highly ordered TiO₂ nanotubes” *Electrochim. Acta*, **54**, 3794-3798.
- Mura, F., Masci, A., Pasquali, M. and Pozio, A. (2010), “Stable TiO₂ nanotube arrays with high UV photoconversion efficiency”, *Electrochimica Acta*, **55**, 2246-2251.
- Oh, S.H., Finñones, R.R., Daraio, C., Chen, L.H. and Jin, S. (2005), “Growth of nano-scale hydroxyapatite using chemically treated titanium oxide nanotubes”, *Biomater.*, **26**(24), 4938-4943.
- Oh, S.H. and Jin, S. (2006) “Titanium oxide nanotubes with controlled morphology for enhanced bone growth”, *Mater. Sci. Eng. C*, **26**, 1301-1306.
- Oh, H.J., Lee, J.H., Kim, Y.J., Suh, S.J., Lee, J.H. and Chi, C.S. (2008), “Surface characteristics of porous anodic TiO₂ layer for biomedical applications”, *Mater. Chem. Phys.*, **109**, 10-14.
- Park, J.H., Kim, S. and Bard, A.J. (2006), “Novel carbon-doped TiO₂ nanotube arrays with high aspect ratios for efficient solar water splitting”, *Nano Lett.*, **6**(1), 24-28.
- Peng, L., Mendelsohn, A.D., LaTempa, T.J., Yoriya, S., Grimes, C.A. and Desai, T.A. (2009), “Long-term small molecule and protein elution from TiO₂ nanotubes”, *Nano Lett.*, **9**(5), 1932-1936.
- Popat, K.C., Eltgroth, M., LaTempa, T.J., Grimes, C.A. and Desai, T.A. (2007a), “Decreased Staphylococcus epidermidis adhesion and increased osteoblast functionality on antibiotic-loaded titania nanotubes”, *Biomater.*, **28**(32), 4880-4888.
- Popat, K.C., Eltgroth, M., LaTempa, T.J., Grimes, C.A. and Desai, T.A. (2007b), “Titania nanotubes: a novel platform for drug-eluting coatings for medical implants?”, *Small*, **3**(11), 1878-1881.
- Pozio, A. (2014), “Effect of low cobalt loading on TiO₂ nanotube arrays for water-splitting”, *Int. J. Electrochem.*, **2014**, 1-7.
- Pozio, A. (2015), “Effect of tantalum doping on TiO₂ nanotube arrays for water-splitting”, *Modern Res. Catal.*, **4**, 1-12.
- Raja, K.S., Misra, M., Mahajan, V.K., Gandhi, T., Pillai, P. and Mohapatra, S.K. (2006), “Photoelectrochemical hydrogen generation using band-gap modified nanotubular titanium oxide in solar light”, *J. Power Sour.*, **161**(2), 1450-1457.
- Sakthivel, S. and Kisch, H. (2003), “Daylight photocatalysis by carbon-modified titanium dioxide”, *Angew. Chem. Int. Ed.*, **42**, 4908-4911.
- Sennik, E., Colak, Z., Kilinc, N. and Ozturk, Z.Z. (2010), “Synthesis of highly-ordered TiO₂ nanotubes for a hydrogen sensor”, *Int. J. Hydro. Energy*, **35**(9), 4420-4427.
- Shankar, K., Tep, K.C., Mor, G.K. and Grimes, C.A. (2006), “An electrochemical strategy to incorporate nitrogen in nanostructured TiO₂ thin films: modification of bandgap and photoelectrochemical properties”, *J. Phys. D, Appl. Phys.*, **39**, 2361-2366.
- Shankar, K., Mor, G.K., Prakasam, H.E., Yoriya, S., Paulose, M., Varghese, O.K. and Grimes, C.A. (2007), “Highly-ordered TiO₂ nanotube arrays up to 220 μm in length: use in water photoelectrolysis and dye-sensitized solar cells”, *Nanotech.*, **18**, 065707.
- Shrestha, N.K., Yang, M., Nah, Y.C., Paramasivam, I. and Schmuki, P. (2010), “Self-organized TiO₂ nanotubes: visible light activation by Ni oxide nanoparticle decoration”, *Electrochem. Commun.*, **12**, 254-257.
- Simmons, E.L. (1975), “Diffuse reflectance spectroscopy: a comparison of the theories”, *Appl. Opt.*, **14**,

1380-1386.

- Su, Y., Han, S., Zhang, X., Chen, X. and Lei, L. (2008) "Preparation and visible-light-driven photoelectrocatalytic properties of boron-doped TiO₂ nanotubes", *Mater. Chem. Phys.*, **110**(2/3), 239-246.
- Surendranath, Y., Kanan, M.W. and Nocera, D.G. (2010), "Mechanistic studies of the oxygen evolution reaction by a cobalt-phosphate catalyst at neutral pH", *J. Am. Chem. Soc.*, **132**, 16501-16509.
- Varghese, O.K., Gong, D., Paulose, M., Ong, K.G., Dickey, E.C. and Grimes, C.A. (2003a), "Extreme changes in the electrical resistance of titania nanotubes with hydrogen exposure", *Adv. Mater.*, **15**(7-8), 624-627.
- Varghese, O.K., Gong, D., Paulose, M., Ong, K.G. and Grimes, C.A. (2003b), "Hydrogen sensing using titania nanotubes", *Sens. Actuat. B*, **93**(1-3), 338-344.
- Wang, Y., Feng, C., Jin, Z., Zhang, J., Yang, J. and Zhang, S. (2006), "A novel N-doped TiO₂ with high visible light photocatalytic activity", *J. Molecul. Catal. A, Chem.*, **260**, 1-3.
- Wang, Y., Yang, H., Liu, Y., Wang, H., Shen, H., Yan, J. and Xu, H. (2010), "The use of Ti meshes with self-organized TiO₂ nanotubes as photoanodes of all-Ti dye-sensitized solar cells", *Prog. Photovol. Res. Appl.*, **18**, 285-290.
- Wu, G., Nishikawa, T., Ohtani, B. and Chen, A. (2007), "Synthesis and characterization of carbon-doped TiO₂ nanostructures with enhanced visible light response", *Chem. Mater.*, **19**(18), 4530-4537.
- Xu, J., Yanhui, A., Chen, M. and Fu, D. (2010), "Photoelectrochemical property and photocatalytic activity of N-doped TiO₂ nanotube arrays", *Appl. Surf. Sci.*, **256**, 4397-4401.
- Yamada, Y., Matsuki, N., Ohmori, T., Mametsuka, H., Kondo, M. and Matsuda, A. (2003), "One chip photovoltaic water electrolysis device", *Int. J. Hydro. Energy*, **28**, 1167-9.
- Yang, J., Wang, D., Han, H. and Li, C. (2013), "Roles of cocatalysts in photocatalysis and photoelectrocatalysis", *Account. Chem. Res.*, **46**(8), 1900-1909.
- Yoldas, B.E. and Partlow, D.P. (1985), "Formation of broad band antireflective coatings on fused silica for high power laser applications", *Thin Solid. Film.*, **129**, 1-14.

PM